

# Locked and Unlocked Chains of Planar Shapes\*

Robert Connelly  
Cornell University  
Ithaca, NY 14853, USA

Erik D. Demaine  
MIT CSAIL  
Cambridge, MA 02139, USA

Martin L. Demaine  
MIT CSAIL  
Cambridge, MA 02139, USA

Sándor P. Fekete  
TU Braunschweig  
D-38106 Braunschweig, Germany

Stefan Langerman  
Université Libre de Bruxelles  
ULB CP212, Belgium

Joseph S. B. Mitchell  
Stony Brook University  
Stony Brook, NY 11794, USA

Ares Ribó  
Freie Universität Berlin  
D-14195 Berlin, Germany

Günter Rote  
Freie Universität Berlin  
D-14195 Berlin, Germany

*Dedicated to Godfried Toussaint  
on the occasion of his 60th birthday.*

## ABSTRACT

We extend linkage unfolding results from the well-studied case of polygonal linkages to the more general case of linkages of polygons. More precisely, we consider chains of nonoverlapping rigid planar shapes (Jordan regions) that are hinged together sequentially at rotatable joints. Our goal is to characterize the families of planar shapes that admit *locked chains*, where some configurations cannot be reached by continuous reconfiguration without self-intersection, and which families of planar shapes guarantee *universal foldability*, where every chain is guaranteed to have a connected configuration space. Previously, only obtuse triangles were known to admit locked shapes, and only line segments were known to guarantee universal foldability. We show that a surprisingly general family of planar shapes, called *slender adornments*, guarantees universal foldability: roughly, the inward normal from any point on the shape's boundary should intersect the line segment connecting the two incident hinges. In contrast, we show that isosceles triangles with any desired apex angle  $< 90^\circ$  admit locked chains, which is precisely the threshold beyond which the inward-normal property no longer holds.

\*R. Connelly supported in part by NSF grant DMS-0209595. E. Demaine supported in part by NSF grant CCF-0347776 and DOE grant DE-FG02-04ER25647. S. Langerman is Chercheur qualifié du FNRS. J. Mitchell supported in part by NSF (CCR-0098172, ACI-0328930, CCF-0431030, CCF-0528209), the U.S.-Israel Binational Science Foundation (2000160), Metron Aviation, and NASA Ames (NAG2-1620).

Permission to make digital or hard copies of all or part of this work for personal or classroom use is granted without fee provided that copies are not made or distributed for profit or commercial advantage and that copies bear this notice and the full citation on the first page. To copy otherwise, to republish, to post on servers or to redistribute to lists, requires prior specific permission and/or a fee.

SCG'06, June 5–7, 2006, Sedona, Arizona, USA.  
Copyright 2006 ACM 1-59593-340-9/06/0006 ...\$5.00.

## Categories and Subject Descriptors

F.2.2 [Nonnumerical Algorithms and Problems]: Geometrical problems and computations

## General Terms

Algorithms, Theory.

## Keywords

Linkages, folding, locked chains, hinged dissections.

## 1. INTRODUCTION

In this paper, we explore the motion-planning problem of *reconfiguring* or *folding* a hinged collection of rigid objects from one state to another while avoiding self-intersection. This general problem has been studied since the beginnings of the motion-planning literature when Reif [14] proved that deciding reconfigurability of a “tree” of polyhedra, amidst fixed polyhedral obstacles, is PSPACE-hard. This result has been strengthened in various directions over the years, although the cleanest versions were obtained only very recently: deciding reconfigurability of a tree of line segments in the plane, and deciding reconfigurability of a chain of line segments in 3D, are both PSPACE-complete [2]. This result is tight in the sense that deciding reconfigurability of a chain of line segments in the plane is easy, in fact, trivial: the answer is always yes [6].

These results illustrate a rather fine line in reconfiguration problems between computationally difficult and computationally trivial. The goal of our work is to characterize what families of planar shapes and hinges lead to the latter outcome, a *universality result* that reconfiguration is always possible. The only known example of such a result, however, is the family of chains of line segments, and that problem was unsolved for about 25 years [6]. Even small perturbations to the problem, such as allowing a single point where three line segments join, leads to *locked* examples where reconfiguration is impossible [5].

What about chains of shapes other than line segments? It is easy to see that a shape tucked into a “pocket” of a non-convex shape immediately makes trivial locked chains with two pieces. Back in January 1998, the third author showed

how to simulate this behavior with convex shapes, indeed, just three triangles; see Figure 1(a). This example has circulated throughout the years to many researchers (including the authors of this paper) who have asked about chains of 2D shapes. The only really unsatisfying feature of the example is that some of the angles are very obtuse. But with a little more work, one can find examples with acute angles, indeed, equilateral triangles, albeit of different size; see Figure 1(b). What could be better than equilateral triangles?

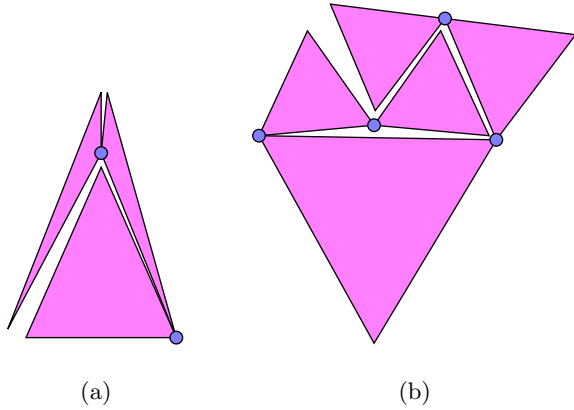


**Figure 1:** Simple examples of locked chains of triangles. (a) A locked chain of three triangles. (b) A locked chain of equilateral triangles of different sizes. The gaps should be tighter than drawn.

It is therefore reasonable to expect, as we did for many years, that there is no interesting class of shapes, other than line segments, with a universality result—essentially all other shapes admit locked chains. We show in this paper, however, that this guess is wrong.

We introduce a family of shapes, called *slender adornments*, and prove that all open and closed chains, made up of arbitrarily many different shapes from this family, can be universally reconfigured between any two states. Indeed, we show that these chains have a natural canonical configuration, analogs of the straight configuration of an open chain and convex configurations of a closed chain. Our result is based on the existence of a particularly strong notion of expansive motions of polygonal chains, called “infinitesimally strictly expansive motions”, proved but not explicitly stated in [6]. Our techniques build on the theory of unfolding chains of line segments, substantially generalizing and extending the results from that theory. Our results go far beyond what *we* thought was possible (until recently).

The family of slender adornments has several equivalent definitions. The key idea is to distinguish the two hinge points on the boundary of the shape connecting to the adjacent shapes in the chain, and view the shape as an *adornment* to the line segment connecting those two hinges, called the *base*. This view is without loss of generality, but provides additional information relating the shapes and how they are attached to neighbors, which turns out to be crucial to obtaining a universality result. An adornment is *slender* if every inward normal of the shape hits the base. Equivalently, as we show, an adornment is slender if and only if the distance from either endpoint of the base to a point moving along one side of the adornment changes monotonically.

Slender adornments are quite general. Figure 2 shows several examples of slender adornment “halves”. These examples are themselves slender adornments, but also any pair can be joined along their bases to make another slender adornment. Our results imply that one can take any of these slender adornments, link the bases together into a chain in any way that the chain does not self-intersect, and the resulting chain can be unfolded without self-intersection to a straight or convex configuration, and thus the chain can be folded without self-intersection into every configuration.

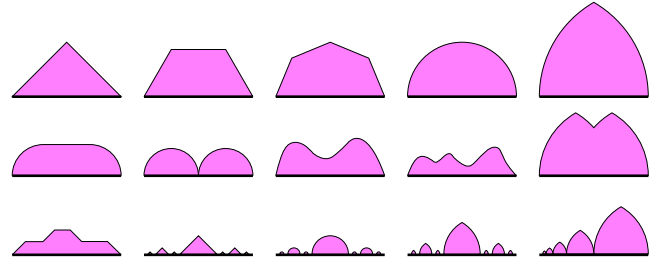


**Figure 2:** Examples of (half of) slender adornments. The base is drawn bold. Any two of these examples could be glued together along a common base.

We also demonstrate the tightness of the family of slender adornments by giving examples of locked chains of shapes that are not slender. Specifically, we show that, for any desired angle  $\theta < 90^\circ$ , there is a locked chain of isosceles triangles with apex angle  $\theta$ . This is precisely the family of isosceles-triangle adornments that are not slender. Thus, for chains of triangles, obtuseness is really desirable, contrary to our intuition from Figure 1(a): the key is that the apex angle opposite the base (in the adornment view) be nonacute, not any other angle. The proof that our examples are locked use the self-touching theory developed for trees of line segments in [5].

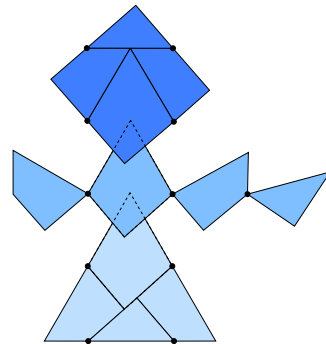


**Figure 3:** Hinged dissection of square to equilateral triangle, described by Dudeney [10]. Different shades show different folded states (overlapping slightly).

**Motivation.** Hinged collections of rigid objects have been studied previously in many contexts, particularly robotics. One recent body of algorithmic work by Cheong et al. [4] considers how chains of polygonal objects can be *immobilized* or *grasped* by a robot with a limited number of actuators. Grasping is a natural first step toward robotic *manipulation*, but the latter challenge requires a better understanding of reconfigurability. This paper offers the first theoretical

underpinnings for reconfiguration of chains of rigid objects (other than line segments).

Another potential application is to continuous folding of hinged dissections. Hinged dissections are chains or trees of polygons that can be reconfigured into two or more self-touching configurations with desired silhouettes. For example, Figure 3 shows a classic hinged dissection from 1902 of a square into an equilateral triangle of the same area. Many general families of hinged dissections have been established in the recent literature [1, 8, 9, 11, 12]. One problem not addressed in this literature, however, is whether the reconfigurations can actually be executed without self-intersection, as in Figure 3. Our results provide potential tools, previously lacking, for addressing this problem. While hinged dissections have frequently been considered in recreational contexts, they have recently found applications in nanomanufacturing [13] and reconfigurable robotics [9].

**Outline.** This paper is organized as follows. Section 2 defines the model and slender adornments more precisely, and proves several basic properties. Section 3 describes the necessary background from unfolding chains of line segments, for proving in Section 4 that chains of slender adornments can always be unfolded. Section 5 describes our examples of locked chains of isosceles triangles, including the necessary background from self-touching trees.

## 2. SLENDER ADORNMENTS

This section provides a formal statement of the objects we consider—adorned chains consisting of slender adornments—and and proves several basic results about them.

### 2.1 Adorned Chains

Our object of study is a chain of nonoverlapping rigid planar shapes (Jordan regions) that are hinged together sequentially at rotatable joints. Another way to view such a chain is to consider the *underlying polygonal chain* of line segments connecting successive joints. (For an open chain, there is some freedom in choosing the endpoints for the first and the last bar of the chain.) On the one hand, these line segments can be viewed as *bars* that move rigidly with the shapes to which they belong. On the other hand, the shapes can be viewed as “adornments” to the bars of an underlying polygonal chain. This view leads to the concept of an “adorned polygonal chain” which we now proceed to define more precisely.

An *adornment* is a simply connected compact region in the plane, called the *shape*, together with a line segment  $ab$  connecting two boundary points, called the *base*. There are two *boundary arcs* from  $a$  to  $b$  which enclose the shape, called *sides*. We require the base to be contained in the shape. (In other words, the base must be a chord of the shape.)

An *adorned polygonal chain* is a set of nonoverlapping adornments whose bases form a polygonal chain. We permit the shapes to touch on their boundary and to slide along each other. However, we require the underlying polygonal chain to be strictly simple: the bases of two shapes are not allowed to touch except at common hinges of the polygonal chain.

The viewpoint of a chain of shapes as an adorned polygonal chain is useful for two reasons. First, we can more easily talk about the kind of shapes, and their relation to the locations of the incident hinges, in a family of chains:

this information is captured by the adornments. Second, the underlying polygonal chain provides a mechanism for folding the chain of shapes, as well as a natural *unfolding* goal: straighten the underlying open chain or convexify the underlying closed chain. Indeed, we show that, in some cases, unfolding motions of the polygonal chain induce valid unfolding motions of the chain of shapes.

### 2.2 Slender Adornments

The class of adornments that we treat have additional regularity requirements on their boundary: we require that each side of the boundary is differentiable except at a countable number of points, and that one-sided (clockwise and counterclockwise) tangents exist everywhere. This class essentially describes all piecewise-smooth shapes with countably many smooth pieces and well-behaved joints between the pieces. We categorize boundary points into two types, *smooth points* and *corners*, according to whether the boundary is differentiable at that point.

We can define the *angle* of a boundary point  $x$  to be the angle of the counterclockwise wedge from the counterclockwise tangent ray of  $x$  to the clockwise tangent ray of  $x$ . See Figure 4. Any line that passes through  $x$  and is either entirely inside or entirely outside this wedge is called a *tangent line*; the pencil of tangent lines includes at its extremes the two lines extending the two tangent rays of  $x$ . At a smooth boundary point  $x$ , the clockwise and counterclockwise tangent rays lie in opposite directions along a common line, the sole tangent line, and the angle of  $x$  is always  $180^\circ$ .

Slenderness requires the notion of “inward normals” of a boundary point  $x$ . The two *primary inward normals* at  $x$  are the rays emanating from  $x$  obtained by rotating the clockwise tangent vector of  $x$  clockwise  $90^\circ$  and by rotating the counterclockwise tangent vector of  $x$  counterclockwise  $90^\circ$ . More generally, an *inward normal* is a ray emanating from  $x$  in the convex wedge formed by the primary inward normals, or equivalently, that is perpendicular to a tangent line and whose direction lies in the same semicircle as the two primary inward normals.

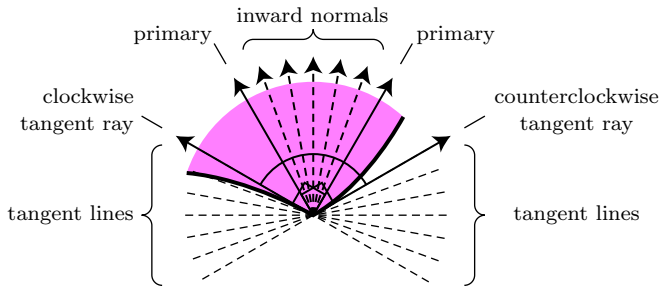
We call an adornment *slender* if every inward normal of the shape intersects the base (possibly at the base’s endpoints). Figure 2 shows examples of slender adornments. In particular, such a shape cannot have any strictly acute corners. As we show in the next section, this condition has two equivalent formulations: (1) requiring just that every *primary* inward normal of the shape intersects the base, and (2) requiring that the distance between an endpoint of the base and a point moving along either side of the shape changes monotonically. Also, we characterize the largest slender adornment (in the partial order defined by set containment) as the crescent enclosed by the two circles centered at one endpoint of the base and passing through the other endpoint of the base.

### 2.3 Basic Properties

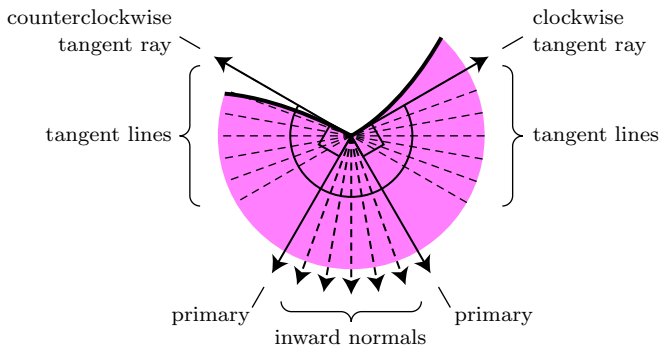
In this section we prove some basic results about when adornments are slender. We begin with the simple equivalence between constraining all inward normals and just primary inward normals:

**LEMMA 1.** *An adornment is slender if and only if every primary inward normal of the shape hits the base.*

An equivalent characterization of slender adornments con-



(a) Convex corner.



(b) Reflex corner.

**Figure 4:** Tangents and inward normals at a corner boundary point. In each case, the circular arc shows the angle of the corner.

strains the distance between an endpoint of the base and a point along the boundary of the shape:

**LEMMA 2.** *An adornment is slender if and only if, for a point moving on either side of the shape, the distance to each endpoint of the base changes monotonically.*

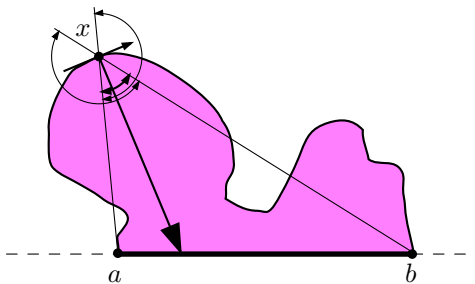


**Figure 5:** The monotone-distance property for slender shapes.

**PROOF.** Let  $x(s)$  be a clockwise arc-length parameterization of a side, starting at one base endpoint  $a$  and ending at the other base endpoint  $b$ . By the assumptions, the distance

function  $f(s) = \|x(s) - a\|$  is smooth except at a countable set of points. The directions of the clockwise and counterclockwise tangents at  $x(s)$  determine the sign of the left and right derivatives  $f'_-(s)$  and  $f'_+(s)$ , via a straightforward geometric relation (see Figure 5):  $f'_+(s) \geq 0$  if and only if the inward normal to the clockwise tangent at  $x$  points into the halfspace to the right of the line  $ax$ , and similarly for  $f'_-(s)$ .

Thus, monotonicity of  $f$  is equivalent to the condition that the primary inward normals lie in the  $180^\circ$  range of directions on one side of the line  $xa$ . Similarly, monotonicity of the distance from  $b$  means that the inward normals point into the halfspace to the left of the line  $bx$ . Together, this is equivalent to the condition that the primary inward normals intersect the base segment  $ab$ .  $\square$

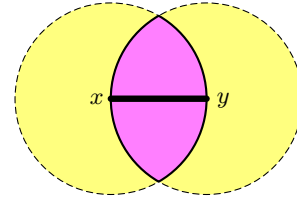


**Figure 6:** The largest slender adornment with a given base is a crescent.

This lemma allows us to determine the largest (in the partial order defined by set containment) possible shape of a slender adornment:

**COROLLARY 3.** *The shape of a slender adornment is contained in the crescent enclosed by the two circles centered at one endpoint of the base and passing through the other endpoint of the base.*

**PROOF.** Refer to Figure 6. Let  $x$  and  $y$  be the two endpoints of the adornment's base. Let  $p$  be a point moving from  $x$  to  $y$  along one of the adornment's sides. At the beginning,  $p = x$ , the distance  $\|x - p\|$  is 0. At the end,  $p = y$ , the distance  $\|x - p\|$  is  $\|x - y\|$ . By Lemma 2, at all times in between,  $\|x - p\|$  must be between 0 and  $\|x - y\|$ . Therefore, all points  $p$  along the boundary of the adornment's shape must be inside or on the circle centered at  $x$  and passing through  $y$ . By symmetry, all such points  $p$  must also be inside or on the circle centered at  $y$  and passing through  $x$ . Therefore all such points  $p$  must be inside or on the boundary of the crescent enclosed by these two circles.  $\square$

The containment partial order on slender adornments in fact forms a lattice with join and meet operators:

**LEMMA 4.** *Slenderness of adornments with the same base is closed under union and intersection.*

### 3. EXPANSIVE MOTIONS OF POLYGONAL CHAINS

Unfoldability of polygonal chains is established in [6] using "expansive" motions. We use a particularly strong notion of expansiveness, called infinitesimal strict expansiveness, which follows from the results of [6] although it is not explicitly mentioned in that paper. In contrast, other approaches to linkage unfolding cannot guarantee infinitesimal strict expansiveness: the motions of [15] satisfy a somewhat weaker

condition (expansiveness), and the motions of [3] satisfy a much weaker condition (energy monotonicity).

We begin with the definition of motions and strict expansiveness, which are the main notions considered in [6]. A *motion* of a polygonal chain is an assignment, for each vertex  $v$  of the chain, of a continuous function  $v(t)$  mapping any time  $t \in [0, 1]$  to a point, representing the location of vertex  $v$  at time  $t$ . A valid motion must satisfy that the length  $\|v(t) - w(t)\|$  of each bar  $\{v, w\}$  is constant over all time  $t \in [0, 1]$ . A motion is *strictly expansive* if every distance  $\|v(t) - w(t)\|$  is a strictly increasing function of time  $t$  up until the time at which  $v(t)$  and  $w(t)$  are connected by a straight chain of bars, after which the distance is constant.

The main result of [6], restricted to the case of a single polygonal chain, is as follows:

**THEOREM 5.** [6, Theorem 1] *Every strictly simple polygonal chain has a piecewise-differentiable strictly expansive motion to a straight or convex configuration.*

The “piecewise-differentiable” property hints at a stronger notion of strict expansiveness, which is what we need. A motion of a polygonal chain is *piecewise differentiable* if the derivative  $dv(t)/dt$  of the motion  $v(t)$  of every vertex  $v$  of the chain is defined at all but finitely many times  $t$ . While the derivative of a piecewise-differentiable motion is not defined at all times  $t$ , we can sometimes define the *forward derivative*  $dv(t)/dt^+$  at any time  $t < 1$  by taking the limit from the positive side:  $dv(t)/dt^+ = \lim_{h \rightarrow 0^+} \frac{v(t+h) - v(t)}{h}$ . We call  $dv(t)/dt^+$  the *velocity vector* of vertex  $v$  at time  $t$ . A motion is *forward differentiable* if the velocity vector  $dv(t)/dt^+$  of every vertex  $v$  is defined for all times  $t < 1$ .

A forward-differentiable motion is *infinitesimally strictly expansive* if, for every two vertices  $v$  and  $w$ , and for any time  $t$  at which  $v$  and  $w$  are not connected by a straight chain of bars, the forward derivative of their Euclidean distance is strictly positive at time  $t$ :  $d\|v(t) - w(t)\|/dt^+ > 0$ . Equivalently, a motion is infinitesimally strictly expansive if, for every two vertices  $v$  and  $w$ , and for any time  $t$  at which  $v$  and  $w$  are not connected by a straight chain of bars, we have

$$\left( \frac{dv(t)}{dt^+} - \frac{dw(t)}{dt^+} \right) \cdot (v(t) - w(t)) > 0. \quad (1)$$

Theorem 5 can be strengthened as follows:

**THEOREM 6.** [6] *Every strictly simple polygonal chain has a forward-differentiable infinitesimally strictly expansive motion to a straight or convex configuration.*

**PROOF.** Theorem 5 shows the existence of a strictly expansive motion, but such a motion could strictly increase a distance between two vertices only to the second order, so that the forward derivative of the distance is zero instead of positive. However, [6] proves the theorem by showing that a system with constraints stronger than (1), namely, (7–10) of [6], has a solution. Therefore, the proof in fact establishes the desired stronger result.  $\square$

In fact, a strictly expansive motion not only increases vertex-to-vertex distances, but it also increases point-to-point distances:

**LEMMA 7.** [6] *Any infinitesimally strictly expansive motion of a polygonal chain has a strictly positive forward derivative  $d\|p(t) - q(t)\|/dt^+$  for any time  $t < 1$  and for any two*

*points  $p$  and  $q$  not connected by a straight chain of bars, where each of  $p$  and  $q$  is chosen to be a vertex or a fixed position along a bar of the chain.*

**PROOF.** A weaker form of this lemma is proved as Corollary 1 of [6], but the same argument applies. At a high level, it suffices to prove the lemma when  $p$  is a vertex and  $q$  is along a bar; then the general lemma can be obtained by applying this case twice. Lemma 1 of [6] shows that the distance  $\|p(t) - q(t)\|$  never decreases, and gives an exact condition of when it does not increase, which cannot hold if  $p$  and  $q$  are not connected by a straight chain of bars. The proof of Lemma 1 of [6] can easily be generalized to show that the forward derivative is positive in the same situation.  $\square$

Our proofs of unfoldability of chains of slender adornments crucially use both Theorem 6 and Lemma 7.

## 4. SLENDER ADORNMENTS CANNOT LOCK

In this section we prove our main positive result:

**THEOREM 8.** *A strictly simple polygonal chain adorned by slender adornments can always be straightened or convexified.*

**PROOF.** We claim that any infinitesimally strictly expansive motion of the underlying polygonal chain straightens or convexifies the adorned chain without self-intersection. Combining this claim with Theorem 6 then proves the theorem.

Suppose for contradiction that two slender adornments intersect in their interiors during an infinitesimally strictly expansive motion of the underlying polygonal chain. Let  $T$  denote the set of times at which two slender adornments intersect in their interiors. By continuity and because the adornment interiors are open sets,  $T$  is a disjoint union of open intervals, and therefore open. Let  $\inf T$  denote the infimum of  $T$ ; here we parameterize time between 0 and 1, so by the least-upper-bound property of  $\mathbb{R}$ ,  $T$  has an infimum. By the approximation property of  $\inf$  in  $\mathbb{R}$ , there is an infinite sequence  $t'_1 > t'_2 > \dots$  of times in  $T$  whose unique accumulation point is  $\inf T$ . Because there is a finite number of adornments, for some two adornments  $A$  and  $B$ , there is an infinite subsequence  $t_1 > t_2 > \dots$  of times at which  $A$  and  $B$  intersect in their interiors, which must have the same unique accumulation point  $\inf T$ . Associate with each time  $t_i$  a point  $a_i$  of  $A$ 's interior and a point  $b_i$  of  $B$ 's interior that are collocated at time  $t_i$ . By compactness of  $A$  and  $B$ , and therefore compactness of  $A \times B$ , the infinite sequence  $(a_1, b_1), (a_2, b_2), \dots$  of points in  $A \times B$  has an accumulation point  $(p_A, p_B)$  in  $A \times B$ . By continuity of the motion,  $p_A$  and  $p_B$  must be collocated at time  $\inf T$ , say at a point  $p$  in the plane. Because  $T$  is open, the interiors of  $A$  and  $B$  do not intersect at time  $\inf T$ , so  $p_A$  and  $p_B$  must be points on the boundaries of  $A$  and  $B$ , respectively.

At time  $\inf T$ ,  $A$  and  $B$  touch at point  $p$  but have disjoint interiors. If the angle of  $p_A$  on  $A$  and the angle of  $p_B$  on  $B$  are both nonreflex, then  $A$  and  $B$  have a common tangent line  $\ell$  through  $p$ . See Figures 7(a) and 7(b). This tangent line  $\ell$  induces an inward normal of  $A$  at  $p$  and an inward normal of  $B$  at  $p$ , pointing in opposite directions. Because

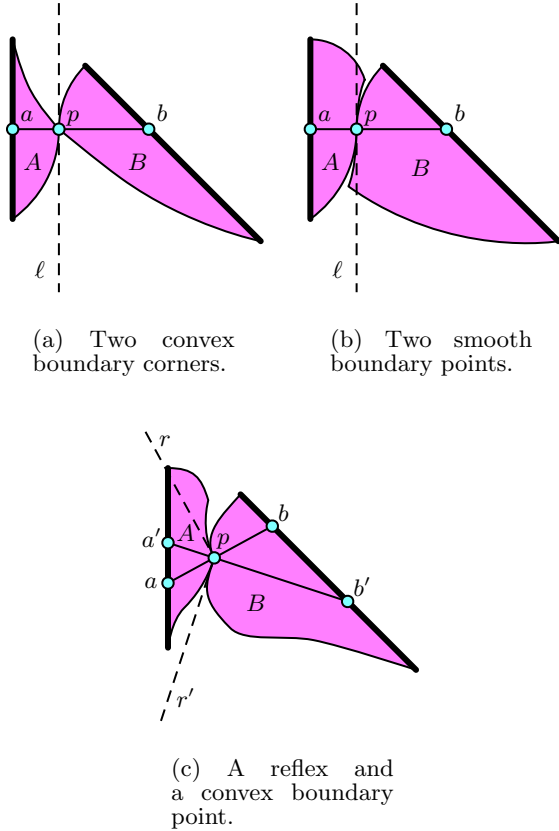


**Figure 7:** Two slender adornments  $A$  and  $B$  touching on the boundary at  $p$ .

$A$  and  $B$  are slender, these inward normals meet their bases, say at points  $a$  and  $b$ , respectively. Rotate the diagram so that  $\ell$  is vertical and  $A$  is left of  $B$ ; thus,  $a$ ,  $p_A$ ,  $p_B$ , and  $b$  are ordered left to right along a horizontal line.

We would like to apply Lemma 7 to argue that the motion strictly increases the distance between  $a$  and  $b$  to the first order at time  $\inf T$ :  $d\|a - b\|/dt|_{t=\inf T} > 0$ . However, Lemma 7 does not apply when  $a$  and  $b$  are connected by a (horizontal) straight chain of bars in the underlying polygonal chain (including the special case when  $a = b$ ). We handle this situation separately. Assume by symmetry that the chain is (just) above  $A$  and  $B$ . By expansiveness, the chain must move rigidly as a unit. Consider the motion of  $A$  and  $B$  relative to the chain (viewing the chain as pinned to the plane):  $A$  can rotate clockwise around  $a$ , and  $B$  can rotate counterclockwise around  $b$ . During any such motion, any point of  $A$  moves clockwise along a circular arc centered at  $a$ , and any point of  $B$  moves counterclockwise along a circular arc centered at  $b$ . Because  $a$  and  $b$  are base endpoints of the slender adornments  $A$  and  $B$ , respectively, by Lemma 2 these circular arcs must remain within the original positions of  $A$  and  $B$  (at time  $\inf T$ ), respectively, until exiting along the “other side” of  $A$  or  $B$  that is not touching  $B$  or  $A$ . We can bound the extent of this other side of  $A$  as being contained in the clockwise wedge from  $A$ ’s base to the vertical upward ray from  $a$ , and similarly bound the other side of  $B$  as contained in the counterclockwise wedge from

$B$ ’s base to the vertical upward ray from  $b$ . Assuming  $A$ ’s base is not itself horizontal (because in that case no motion of  $A$  is possible in an expansive motion), the other side of  $A$  is bounded away from the vertical ray by some strictly positive angle; and similarly for  $B$ . Thus, for a sufficiently short time interval  $[\inf T, \inf T + \varepsilon)$ , all points in  $A$  and  $B$  remain within the union of the original positions of  $A$  and  $B$ , respectively, and the surrounding wedge to a vertical ray. These regions of confinement have disjoint interiors, so for a sufficiently short time interval  $[\inf T, \inf T + \varepsilon)$ ,  $A$  and  $B$  must keep disjoint interiors. Because  $\inf T$  is an accumulation point, there is an index  $i$  for which  $t_i \in [\inf T, \inf T + \varepsilon)$ . We conclude that  $A$  and  $B$  have disjoint interiors at time  $t_i$ , contradicting that  $a_i$  and  $b_i$  were defined to be interior points of  $A$  and  $B$ , respectively, that are collocated at time  $t_i$ .

Now we return to the case in which we can apply Lemma 7 to conclude that  $d\|a - b\|/dt|_{t=\inf T} > 0$ . Consider the motion of  $A$  relative to  $B$  (pinning  $B$  to the plane), with points  $p_A$  and  $a$  tracking the motion of  $A$ , and with points  $p_B$  and  $b$  remaining fixed, starting at time  $\inf T$ . By the triangle inequality, this distance  $\|a - b\|$  is always at most the sum of the two distances  $\|a - p_A\|$  and  $\|p_A - b\|$ . At time  $\inf T$ , this inequality holds with equality. During the motion, the first distance  $\|a - p_A\|$  remains fixed because both  $a$  and  $p_A$  move relative to  $A$ . Therefore the second distance  $\|p_A - b\|$  must strictly increase to the first order at time  $\inf T$ :  $d\|p_A - b\|/dt|_{t=\inf T} > 0$ . Equivalently, the velocity vector  $v$  of  $p_A$  at time  $\inf T$  must have a strictly negative  $x$  component.

Define the cone  $C$  of directions to consist of a closed interval of directions, containing the direction of  $v$  in its strict interior, such that all directions in  $C$  have a strictly negative  $x$  component. (For example, one such choice of  $C$  is the closed interval of directions between the two bisectors between the direction of  $v$  and the two vertical directions.) Let  $C(q)$  denote the translation of the cone  $C$  to have its apex at point  $q$ . By forward differentiability of  $p_A(t)$ , in any sufficiently small time interval  $[\inf T, \inf T + \varepsilon)$ ,  $p_A(t)$  remains in its original cone  $C(p_A(\inf T))$ . (Here and at other necessary places in the proof, we explicitly write the parameterization of  $p_A$  with respect to time  $t$ .) Because  $A$  moves rigidly, the velocity vector of a point in  $A$  at time  $\inf T$  varies linearly as a function of that point. Thus, points of  $A$  nearby  $p_A$  have a velocity vector at time  $\inf T$  similar to  $v$ . By forward differentiability again, for any sufficiently small time interval  $[\inf T, \inf T + \varepsilon)$ , there is a small enough constant  $\delta > 0$  such that any point  $q$  of  $A$  with  $\|q - p_A\| < \delta$  satisfies that  $q(t)$  remains in its original cone  $C(q(\inf T))$  for the entire time interval  $[\inf T, \inf T + \varepsilon)$ . We can also guarantee that  $q(t)$  remains within a distance of  $2\varepsilon\|v\|$  from its original position  $q(\inf T)$  for the duration of the time interval, because  $q(t)$  travels at a speed of roughly  $\|v\|$  for small enough  $\varepsilon$  and  $\delta$ .

Let  $R(\varepsilon, \delta)$  denote the set of points  $z$  in the plane contained in a cone  $C(q(\inf T))$  and satisfying  $\|z - q(\inf T)\| < 2\varepsilon\|v\|$  for some  $q$  in  $A$  with  $\|q - p_A\| < \delta$ . Because the vertical line  $\ell$  is a common tangent between  $A$  and  $B$  at time  $\inf T$  with  $A$  to the left of  $B$ , and because  $C$  is a closed interval of directions strictly left of vertical,  $R(\varepsilon, \delta)$  is disjoint from the interior of  $B$  for sufficiently small  $\varepsilon > 0$  and  $\delta > 0$ . By the argument above, for any sufficiently small time interval  $[\inf T, \inf T + \varepsilon)$ , there is a small enough constant  $\delta > 0$  such that any point  $q$  of  $A$  with  $\|q - p_A\| < \delta$  satisfies that  $q(t)$  remains in  $R(\varepsilon, \delta)$  for the entire time in-

terval  $[\inf T, \inf T + \varepsilon)$ . However, because  $p_A$  and  $\inf T$  are accumulation points, for any such  $\varepsilon > 0$  and  $\delta > 0$ , there is an index  $i$  such that  $\|a_i - p_A\| < \delta$  and  $t_i \in [\inf T, \inf T + \varepsilon)$ . Therefore, for sufficiently small  $\varepsilon > 0$  and  $\delta = \delta(\varepsilon) > 0$ ,  $a_i(t_i)$  is in  $R(\varepsilon, \delta)$ , contradicting that  $a_i(t_i)$  is interior to  $B$ .

On the other hand, suppose that the angle of  $p_A$  on  $A$  is convex and that the angle of  $p_B$  on  $B$  is reflex. See Figure 7(c). In this case, we consider the clockwise tangent ray  $r$  and the counterclockwise tangent ray  $r'$  of  $B$  at  $p$ . These rays induce the primary inward normals of  $B$  at  $p$ . Suppose they meet  $B$ 's base at points  $b$  and  $b'$ , respectively. Because  $A$  is convex at  $p$  and interior-disjoint from  $B$ , the lines extending  $r$  and  $r'$  are also tangent to  $A$  at  $p$ . Thus, they also induce inward normals of  $A$  at  $p$ , pointing in the opposite directions as the primary inward normals of  $B$  at  $p$ . Suppose they meet  $A$ 's base at points  $a$  and  $a'$ , respectively.

Applying part of the argument from the previous case, twice, we conclude that the velocity vector  $v$  of  $p_A$  at time  $\inf T$  must have positive dot product with both of the inward normals of  $p$  at  $A$ . Equivalently, the velocity vector  $v$  must point strictly interior to the counterclockwise wedge from  $r$  to  $r'$ . Then we can define a cone  $C$  of a closed interval of directions, strictly contained within this counterclockwise wedge and containing the direction of  $v$  in its strict interior. The rest of the argument proceeds as in the previous case: the identically defined region  $R(\varepsilon, \delta)$  is disjoint from the interior of  $B$  for sufficiently small  $\varepsilon > 0$  and  $\delta > 0$ , and for sufficiently small  $\varepsilon > 0$  and  $\delta = \delta(\varepsilon) > 0$ , there is an index  $i$  such that  $a_i(t_i)$  is in  $R(\varepsilon, \delta)$ , contradicting that  $a_i(t_i)$  is interior to  $B$ .  $\square$

## 5. LOCKED CHAINS OF SHARP TRIANGLES

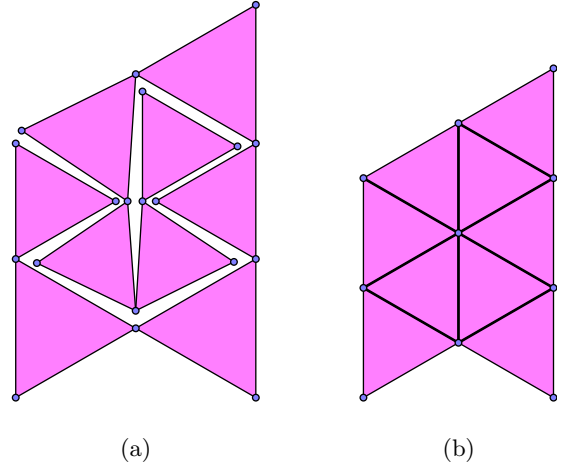
An isosceles triangle with an apex angle of  $\geq 90^\circ$  and with the nonequal side as the base is a slender adornment. By Theorem 8, any chain of such triangles can be straightened. In this section we show that this result is tight: for any isosceles triangle with an apex angle of  $< 90^\circ$  and with the nonequal side as a base, there is a chain of these triangles that cannot be straightened.

Figure 8(a) shows the construction for equilateral triangles (of slightly different sizes). This figure is drawn with the pieces loosely separated, but the actual construction has arbitrarily small separations and arbitrarily closely approximates the self-touching geometry shown in Figure 8(b). Stretching the triangles in this self-touching geometry, as shown in Figure 9, defines our construction for any isosceles triangles with an opposite angle of any value less than  $90^\circ$ . In this case, however, our construction uses two different scalings of the same triangle.

### 5.1 Theory of Self-Touching Configurations

This view of the construction as a slightly separated version of a self-touching configuration allows us to apply the program developed in [5] for proving a configuration locked. This theory allows us to study the rigidity of self-touching configurations, which is easier because vertices cannot move even slightly, and obtain a strong form of lockedness of non-self-touching perturbations drawn with sufficiently small (but positive) separations.

To state this relation precisely, we need some terminology



**Figure 8:** A locked chain of nine equilateral triangles. (a) Drawn loosely. Separations should be smaller than they appear. (b) Drawn tightly, with no separation, as a self-touching configuration.

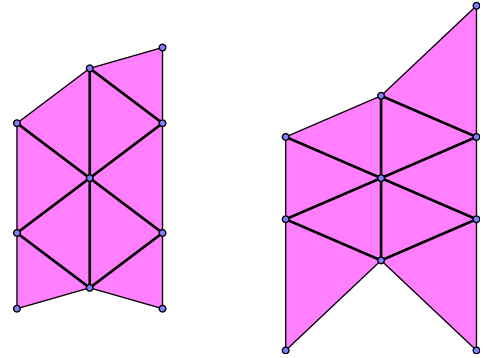


**Figure 9:** Variations on the self-touching configuration from Figure 8(b) to have any desired angle  $< 90^\circ$  opposite the base of each triangle.

from [5]. Call a linkage configuration *rigid* if it cannot move at all. Define a  $\delta$ -*perturbation* of a linkage configuration to be a repositioning of each vertex within distance  $\delta$  of its original position, without regard to preserving edge lengths (better than  $\pm 2\delta$ ), but consistent with the combinatorial information of which vertices are on which side of which bar. Call a linkage *locked within  $\varepsilon$*  if no motion that leaves some bar pinned to the plane moves any point by more than  $\varepsilon$ . Call a self-touching linkage configuration *strongly locked* if, for any desired  $\varepsilon > 0$ , there is a  $\delta > 0$  such that all  $\delta$ -perturbations are locked within  $\varepsilon$ . Thus, if a self-touching configuration is strongly locked, then the smaller we draw the separations in a non-self-touching perturbation, the less the configuration can move. In particular, if we choose  $\varepsilon$  small enough, the linkage must be locked in the standard sense of having a disconnected configuration space.

**THEOREM 9.** [5, Theorem 8.1] *If a self-touching linkage configuration is rigid, then it is strongly locked.*

Therefore, if we can prove that the self-touching configuration in Figure 8(b) (and its variations in Figure 9) are

rigid, then sufficiently small perturbations along the lines shown in Figure 8(a) are rigid.

The theory of [5] also provides tools for proving rigidity of a self-touching configuration. Specifically, we can study *infinitesimal motions* which just define the beginning of a motion to the first order. Call a configuration *infinitesimally rigid* if it has no infinitesimal motions.

LEMMA 10. [5, Lemma 6.1] *If a self-touching linkage configuration is infinitesimally rigid, then it is rigid.*

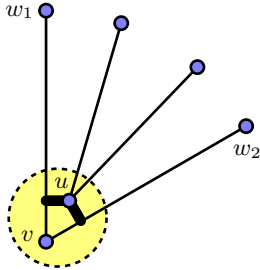


Figure 10: Two zero-length connections between vertices  $u$  and  $v$ .

A final tool we need from [5] is for proving infinitesimal rigidity. For each vertex  $u$  wedged into a convex angle between two bars  $\{v, w_1\}$  and  $\{v, w_2\}$ , we say that there are two *zero-length connections* between  $u$  and  $v$ , one perpendicular to each of the two bars  $\{v, w_i\}$ .<sup>1</sup> See Figure 10. These connections must increase to the first order because  $u$  must not cross the two bars  $\{v, w_i\}$ . In proving infinitesimal rigidity, we can choose to discard any zero-length connections we wish, because ignoring some of the noncrossing constraints only makes the configuration more flexible. Together, the bars and the zero-length connections are the *edges* of the configuration. Define a *stress* to be an assignment of real numbers (*stresses*) to edges such that, for each vertex  $v$ , the vectors with directions defined by the edges incident to  $v$ , and with magnitudes equal to the corresponding stresses, sum to the zero vector. We denote the stress on a bar  $\{v, w\}$  by  $\omega_{vw}$ , and we denote the stress on a zero-length connection between vertex  $u$  and vertex  $v$  perpendicular to  $\{v, w\}$  by  $\omega_{u,vw}$ .

LEMMA 11. [5, Lemma 7.2] *If a self-touching configuration has a stress that is negative on every zero-length connection, and if the configuration is infinitesimally rigid when every zero-length connection is treated as a bar pinning two vertices together, then the self-touching configuration is infinitesimally rigid.*

## 5.2 Locked Chains

We are now in the position to state the precise senses in which the chains of isosceles triangles in Figures 8 and 9 are locked:

THEOREM 12. *The self-touching chains of nine isosceles triangles shown in Figures 8(b) and 9 are rigid provided that the apex angle is  $< 90^\circ$ .*

Applying Theorem 9, we obtain the desired result:

<sup>1</sup>The definition of such connections in [5] is more general, but this definition suffices for our purposes.

COROLLARY 13. *The self-touching chains of nine isosceles triangles shown in Figures 8(b) and 9 are strongly locked provided that the apex angle is  $< 90^\circ$ . Therefore, any sufficiently small non-self-touching perturbation, similar to the one shown in Figure 8(a), is locked.*

Sections 5.3–5.4 prove Theorem 12.

## 5.3 Simplifying Rules

We introduce two rules that significantly restrict the allowable motions of the self-touching configuration of isosceles triangles.

RULE 1. *If a bar  $b$  is collocated with another bar  $b'$  of equal length, and the bars incident to  $b'$  form angles less than  $90^\circ$  on the same side as  $b$ , then any motion must keep  $b$  collocated with  $b'$  for some positive time. See Figure 11.*

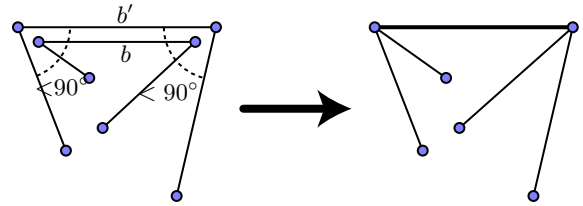


Figure 11: Rule 1 for simplifying self-touching configurations.

PROOF. The noncrossing constraints at the endpoints of  $b$  and  $b'$  prevent  $b$  from moving relative to  $b'$  until the angles at the endpoints of  $b'$  open to  $\geq 90^\circ$ , which can only happen after a positive amount of time.  $\square$

We can apply this rule to the region shown in Figure 12, resulting in a simpler linkage with the same infinitesimal behavior. Although the figure shows positive separations for visual clarity, we are in fact acting on the self-touching configuration of Figure 8(b).

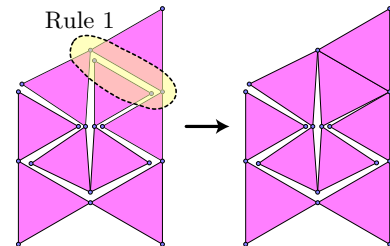


Figure 12: Applying Rule 1 to the chain of nine equilateral triangles from Figure 8.

RULE 2. *If a bar  $b$  is collocated with an incident bar  $b'$  of the same length whose other incident bar  $b''$  forms a convex angle with  $b'$  surrounding  $b$ , then any motion must keep  $b$  collocated with  $b'$  for some positive time. See Figure 13.*

PROOF. The noncrossing constraints at the endpoint of  $b$  surrounded by the convex angle formed by  $b'$  and  $b''$  prevent  $b$  from moving relative to  $b'$  until the convex angle opens to  $\geq 90^\circ$ , which can only happen after a positive amount of time.  $\square$

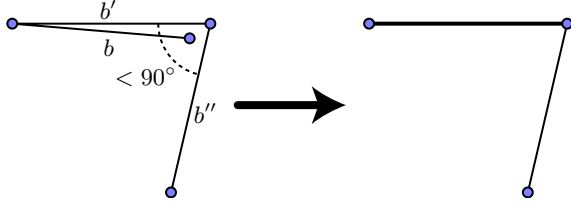


Figure 13: Rule 2 for simplifying self-touching configurations.

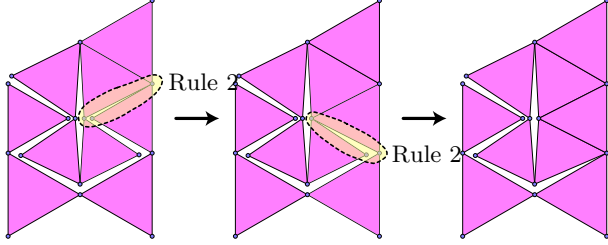


Figure 14: Applying Rule 2 twice to the configuration from Figure 12.

We can apply this rule twice, as shown in Figure 14, to further simplify the linkage.

The final simplification comes from realizing that the central quadrangle gap between triangles is effectively a triangle because the right pair of edges are a rigid unit. Thus the gap forms a rigid linkage (though it is not infinitesimally rigid, because a horizontal movement of the central vertex would maintain distances to the first order), so we can treat it as part of a large rigid block. Figure 15 shows a simplified drawing of this self-touching configuration, which is rigid if and only if the original self-touching configuration is rigid.

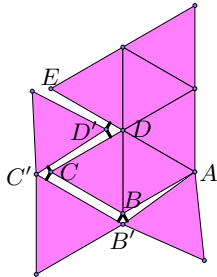


Figure 15: The simplified configuration from Figure 14.

## 5.4 Stress Argument

Finally we argue that the simplified configuration of Figure 15 is infinitesimally rigid using Lemma 11. The configuration is clearly infinitesimally rigid if  $B$  is pinned against  $B'$ ,  $C$  is pinned against  $C'$ , and  $D$  is pinned against  $D'$ . It remains to construct a stress that is negative on all length-zero connections. The stress we construct is nonzero only on the edges connecting points with labels in Figure 15; we also set  $\omega_{AD} = 0$ .

We start by assigning the stresses incident to  $A$ . We choose  $\omega_{AB} < 0$  arbitrarily, and set  $\omega_{AB'} := -\omega_{AB} > 0$ .  $A$  is now in equilibrium because these stress directions are parallel.

We symmetrically assign  $\omega_{BC} := \omega_{AB} < 0$  and  $\omega_{B'C'} = \omega_{A'B'} > 0$ . The resulting forces on  $B$  and  $B'$  are vertical. They can be balanced by an appropriate choice of the

stresses  $\omega_{B,B'A} = \omega_{B,B'C'} < 0$ , which, taken together, also point in the vertical direction.

Vertex  $D'$  has exactly three incident stresses— $\omega_{C'D'}$ ,  $\omega_{D',DC}$ , and  $\omega_{D',DE}$ —which do not lie in a halfplane. Thus there is an equilibrium assignment to these stresses, unique up to scaling, and the stresses all have the same sign. Because zero-length connections must be negative, we are forced to make all three of these stresses negative. We also choose this scale factor to be substantially smaller than the stresses that have been assigned so far.

By assigning  $\omega_{CD} = -\omega_{C'D'}$ , we establish equilibrium at vertex  $D$  as well: the forces at  $D$  are the same as at  $D'$ , only with reversed signs.

Vertex  $C$  feels two stresses assigned so far— $\omega_{CD} > 0$  and  $\omega_{BC} < 0$ . By the choice of scale factors, the latter force dominates, leaving us with a negative force in the direction close to  $CB$ , and two stresses  $\omega_{C,C'B'}$  and  $\omega_{C,C'D'}$  which can be used to balance this force. The three directions do not lie in a halfplane. Therefore  $\omega_{C,C'B'}$  and  $\omega_{C,C'D'}$  can be assigned negative stresses.

Finally, vertex  $C'$  is also in equilibrium because  $\omega_{B'C'} = -\omega_{BC}$ ,  $\omega_{C'D'} = -\omega_{CD}$ , and the stress from the zero-length connections are the same as for  $C$  but in the opposite direction.

In summary, we have shown the existence of a stress that is positive on all zero-length connections. By Lemma 11, the self-touching configuration is infinitesimally rigid, so by Lemma 10, the configuration is rigid. By the simplification arguments above, the original self-touching configuration is also rigid. By Theorem 9, the original self-touching configuration is strongly locked, so sufficiently perturbations are locked.

We remark that an argument similar to the one above, using an assignment of stresses, can also be used for proving Rules 1 and 2, with an appropriate modification of Lemma 11; however, the direct argument that we have given is simpler.

The argument relied on the isosceles triangles having an apex angle of  $< 90^\circ$  (but no more) in order to guarantee that particular triples of stress directions are or are not in a halfplane. It also relies on the symmetry of the configuration through a vertical line (excluding the triangle in the upper right). Thus the argument generalizes to all isosceles triangles sharper than  $90^\circ$ .

## 5.5 Locked Equilateral Triangles

Figure 16 shows another, simpler example of a locked chain of equilateral triangles, using just seven triangles instead of nine. However, this example cannot be stretched into a locked chain of triangles with an arbitrary apex angle of  $< 90^\circ$ , as in Figure 9.

To prove that this example is locked, we first apply Rule 1 and then Rule 2, as shown in Figure 17. Unlike the previous example, the resulting simplified configuration is not infinitesimally rigid (the middle vertex can move infinitesimally horizontally), so we cannot use a stress argument. In this case, however, we can use a more direct argument to prove rigidity of the simplified configuration (and thus of the original self-touching configuration).

Let  $\ell$  denote the side length of the triangles in any of the self-touching configurations. Consider the two dashed chains self-connecting vertices  $A$  and  $B$  in the simplified configuration. The left chain of two bars forces the distance between  $A$  and  $B$  to be at most  $2\ell$ , with equality as in the original

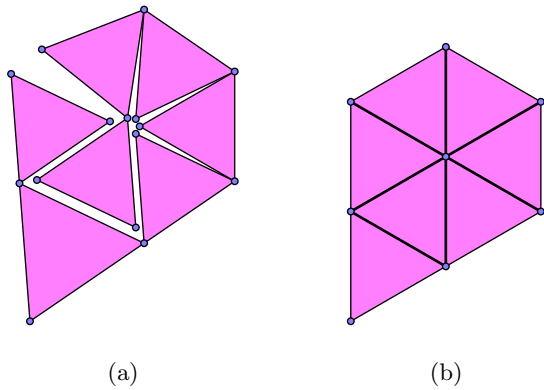


**Figure 16:** A locked chain of seven equilateral triangles. (a) Drawn loosely. Separations should be smaller than they appear. (b) Drawn tightly, with no separation, as a self-touching configuration.

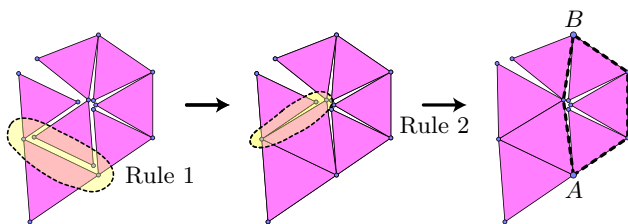


**Figure 17:** Applying Rules 1 and 2 to the chain of seven equilateral triangles from Figure 16.

configuration only if the angle between the two bars remains straight. The right chain of three bars can only open its angles, because of the three triangles on the inside, so the right chain acts as a *Cauchy arm*. The Cauchy-Steinitz Arm Lemma (see, e.g., [7]) proves that the endpoints of such a chain can only get farther away from each other. Thus the distance between  $A$  and  $B$  is at least  $2\ell$ , with equality only if the angles in the right chain do not change. These upper and lower bounds of  $2\ell$  on the distance between  $A$  and  $B$  force the bounds to hold with equality, which prevents any angles from changing except possibly for the angles at  $A$  and  $B$ . However, it is impossible to change fewer than four angles of a closed chain such as the one formed by the left and right dashed chains. (This simple fact was also proved by Cauchy [7].) Therefore, the configuration is rigid.

Applying Theorem 9, we obtain that the self-touching configuration is strongly locked:

**THEOREM 14.** *The self-touching chain of seven equilateral triangles shown in Figure 16(b) is rigid and thus strongly locked. Therefore, any sufficiently small non-self-touching perturbation, similar to the one shown in Figure 16(a), is locked.*

## 6. REFERENCES

[1] J. Akiyama and G. Nakamura. Dudeney dissection of polygons. In *Revised Papers from the Japan Conference on Discrete and Computational Geometry*, volume 1763 of *Lecture Notes in Computer Science*, pages 14–29, Tokyo, Japan, December 1998.

[2] H. Alt, C. Knauer, G. Rote, and S. Whitesides. On the complexity of the linkage reconfiguration problem. In J. Pach, editor, *Towards a Theory of Geometric Graphs*, volume 342 of *Contemporary Mathematics*, pages 1–14. American Mathematical Society, 2004.

[3] J. H. Cantarella, E. D. Demaine, H. N. Iben, and J. F. O’Brien. An energy-driven approach to linkage unfolding. In *Proceedings of the 20th Annual ACM Symposium on Computational Geometry*, pages 134–143, Brooklyn, New York, June 2004.

[4] J.-S. Cheong, A. F. van der Stappen, K. Goldberg, M. H. Overmars, and E. Rimon. Immobilizing hinged polygons. *International Journal of Computational Geometry and Applications*. To appear.

[5] R. Connelly, E. D. Demaine, and G. Rote. Infinitesimally locked self-touching linkages with applications to locked trees. In J. Calvo, K. Millett, and E. Rawdon, editors, *Physical Knots: Knotting, Linking, and Folding of Geometric Objects in 3-space*, pages 287–311. American Mathematical Society, 2002.

[6] R. Connelly, E. D. Demaine, and G. Rote. Straightening polygonal arcs and convexifying polygonal cycles. *Discrete & Computational Geometry*, 30(2):205–239, September 2003.

[7] P. R. Cromwell. Equality, rigidity, and flexibility. In *Polyhedra*, chapter 6, pages 219–247. Cambridge University Press, 1997.

[8] E. D. Demaine, M. L. Demaine, D. Eppstein, G. N. Frederickson, and E. Friedman. Hinged dissection of polyominoes and polyforms. *Computational Geometry: Theory and Applications*, 31(3):237–262, June 2005.

[9] E. D. Demaine, M. L. Demaine, J. F. Lindy, and D. L. Souvaine. Hinged dissection of polypolyhedra. In *Proceedings of the 9th Workshop on Algorithms and Data Structures*, volume 3608 of *Lecture Notes in Computer Science*, pages 205–217, Waterloo, Canada, August 2005.

[10] H. E. Dudeney. Puzzles and prizes. *Weekly Dispatch*, 1902. The puzzle appeared in the April 6 issue of this column, and the solution appeared on May 4.

[11] D. Eppstein. Hinged kite mirror dissection. arXiv:cs.CG/0106032, June 2001.

[12] G. N. Frederickson. *Hinged Dissections: Swinging & Twisting*. Cambridge University Press, August 2002.

[13] C. Mao, V. R. Thallidi, D. B. Wolfe, S. Whitesides, and G. M. Whitesides. Dissections: Self-assembled aggregates that spontaneously reconfigure their structures when their environment changes. *Journal of the American Chemical Society*, 124:14508–14509, 2002.

[14] J. H. Reif. Complexity of the mover’s problem and generalizations. In *Proceedings of the 20th Annual IEEE Symposium on Foundations of Computer Science*, pages 421–427, 1979.

[15] I. Streinu. A combinatorial approach to planar non-colliding robot arm motion planning. In *Proceedings of the 41st Annual Symposium on Foundations of Computer Science*, pages 443–453, Redondo Beach, California, November 2000.